RSC Advances

ROYAL SOCIETY OF CHEMISTRY

www.rsc.org/advances

Facile fabrication of superhydrophobic Titanium surface with mechanical durability by chemical etching

Xiaojia Gao[1], Wenjian Tong[1], Xiaoping Ouyang[1,2], Xiufeng Wang[1,2*]

[1] *School of Materials Science and Engineering, Xiangtan University, Hunan 411105, China*

[2] *National-Provincial Laboratory of Special Function Thin Film Materials, Xiangtan University, Hunan 411105, China*

*Author to whom correspondence should be addressed. Email: onexf@xtu.edu.cn

Phone: 86-732-58298518; Fax: 86-732-58298518

Improving the mechanical durability is crucial to the superhydrophobic metal surfaces. Here we present a simple and efficient method to fabricate stable superhydrophobic Titanium surface with good stretch resistance. Farmland-like textures are generated on Titanium surface by means of chemical etching method. The effects of reaction conditions on the surface wettability and morphology of the prepared surfaces are determined by scanning electron microscopy, X-ray diffraction and contact angle measurement. Furthermore, the mechanical durability of superhydrophobic Titanium surface are examined by tension test, and the relationship among wettability, roughness and tensile strain for superhydrophobic Titanium surface are analyzed. The result shows that the best fabricated superhydrophobic surface not only exhibits good superhydorphobicity (with a water contact angle of 164 ± 1^0 together with a water tilting angle of about 2^0), but also possesses remarkable stretch resistance. Our proposed method will provide guidance in developing facile superhydrophobic metal surfaces with good mechanical durability.

Keywords: superhydrophobic sufaces, Titanium, chemical etching and self-assembly, tensile strain

1. Introduction

Wettability is an important property of a solid surface, mainly associated with the microstructure and surface free energy[1]. Superhydrophobic surfaces with a water contact angle greater than 150° have attracted a great deal of attention in scientific research owing to their excellent performance, such as self-cleaning effect[2-4], anti-resistance[5,6], anti-erosion[7,8] and anti-icing[9-11]. These properties could be achieved by a rough microstructure and a low surface energy.

So far, a great variety of superhydrophobic surfaces based on wood[12-14], glass[15-17], metal[18-20], cloth[21-23], polymer[24,25] as well as bioinspired surfaces[26-33] have been fully investigated. Among these materials, metallic superhydrophobic surfaces have attracted significant interest due to their technological applicability and easy control of morphology. For example, Su *et al.*[34] fabricated the pine-like structure of nickel on copper substrate by an electrodeposition technique. The as-prepared superhydrophobic surface exhibited good chemical stability in both acidic and alkaline environments. Yang *et al.*[35] used hydrochloric acid to prepare superhydrophobic aluminium alloy surfaces with a contact angle of 160˚ and a small roll angle of 4˚. In particular, the obtained superhydrophobic surfaces exhibit remarkable anti-erosion characteristics. Li *et al.*[36] constructed a superhydrophobic zinc surface with loose-stacked ZnO nanorods by hydrothermal oxidation, which can reduce the zinc corrosion rate to about one-eighth of the untreated surface.

As one of the common metals, Titanium is widely used in aerospace, navigation, biomedicine due to its high specific strength, corrosion resistance, biocompatibility. Many methods have been developed to fabricate superhydrophobic Titanium surfaces due to its great potential for industrial applications. For instance, Guo *et al.*[37] fabricated dendritic-like Ti_2O superhydrophobic surface on the Titanium substrate by thermal oxidation and self-assembly modification, which exhibits outstanding chemical stability and mechanical durability. Fadeeva *et al.*[38] obtained superhydrophobic Titanium surfaces using femtosecond laser ablation in a single

processing step, which possesses a surface topography mimicking the lotus leaf. However, the existing methods require rigid conditions and expensive materials in which the processes are time-consuming for multi-steps. Specifically, the mechanically durability of those superhydrophobic surfaces haven't been examined yet. Therefore, it is necessary to develop some simple and effective methods to obtain superhydrophobic surfaces with mechanical stability. Herein, we report a facile method based on chemical etching and surface self-assembly to fabricate stable superhydrophobic Titanium surfaces with farmland-like texture, and these superhydrophobic surfaces show significant mechanical durability by the surface tension test.

2. Materials and methods

2.1. Materials and preparation of superhydrophobic Titanium surfaces

Square Titanium plates (99.9%; Hunan golden days of Titanium industry technology Co., LTD, China) with a size of 10 mm and thickness of 2 mm were firstly surface polished with sandpapers of 120#, 400#, 800#, 1200#, respectively, then ultrasonically cleaned with ethanol, acetone and ultrapure water for 10 min respectively. Next, the cleaned specimens were dried at temperature of 80^{o}C for 15min. A series of H_2SO_4 (aq) with a certain mass fraction (from 32% to 92%) were prepared using analytically pure H_2SO_4 reagent (95%-98%, Hengyang kaixin chemical reagent Co., LTD, China). The reaction kettle equipped with prepared Titanium specimens and H_2SO_4 reagent were put in the thermotank at a given temperature (from 80 ^{o}C to 160 ^{o}C) for a certain time (from 10 minutes to 120 minutes). After that, they were cooled at room temperature for one hour. Subsequently, the samples were ultrasonically cleaned with ethanol, acetone and ultrapure water for 10 min respectively and dried at ambient temperature. Finally, the Titanium specimens were immersed into the 1wt% methanol solution of 1H, 1H, 2H, 2H-Perfluorodecyltrichlorosilane (FDTS) for one hour and then heated at 80^{o}C for 30 minutes. Thus, superhydrophobic Titanium surfaces were obtained.

2.2. Surface characterization

SEM (Phenom, Netherlands) was used to characterize the microstructure of the chemical etching specimens. The accelerate voltage is 5 KV and the accuracy is 17 nm. XRD (D8 Focus, Germany) analysis was carried out to examine the chemical composition of the treated specimens. Using contact angle tester (Rame-hart Instrument Co., USA) to determine the sample superhydrophobic performance, the water volume for testing was 10 μL. The water contact angle (WCA) was measured at five different points of each sample.

2.3. Tension tests

To perform the tension test, the superhydrophobic sample is made into a standard I-shape and size. All tension tests are performed by using a tension testing machine (RG-2000, China). The samples were stretched at the strain rate of 1.67×10^{-4} $N\cdot S^{-1}$ until reaching the specified deformation. Then, holding the same load for one minute and unloading with a rate of 8 $N\cdot S^{-1}$ are performed, respectively. The machine is designed to read the load required to maintain this uniform stretching. The water contact angles of the superhydrophobicity surfaces were measured again after the tension test.

3. Results and discussion

3.1. Sample chemical structure

Figure 1 shows the XRD spectrum of Titanium plate sample before and after the chemical etching. The peak of the plate sample before etching is well corresponded to hexangular Titanium (JCPDS 44-1294). Except for hexangular Titanium, the weak peaks of TiO (JCPDS 09-0240) can be detected in the specimen after the chemical etching, and the XRD spectrum for different etching conditions are basically consistent. The results indicated that Titanium was partially oxidized by H_2SO_4 solution in the process of cooling, and TiO would react with moisture in the environment and generate hydroxyl groups. The hydrolyzed FDTS molecules would

be condensed with these hydroxyl groups to form molecular bonds, which is helpful to improve the stability of superhydrophobic film.

3.2. Surface wettability

Surface wettability of the samples was evaluated by WCA measurements. Fig. 2(a) shows the optical image of water droplet behavior on as-prepared Titanium substrate, it has hydrophilic properties with a contact angle of 72° ± 3°. Fig. 2(b) displays the shape of a water droplet on the as-prepared Titanium substrate after etched at a solution containing 72% H_2SO_4 at 120℃ for 30 minutes, and the static WCA is found to be 36° ± 2°, indicating that surface hydrophilicity can be enhanced to superhydrophilicity by creating both nano- and microtextures. This is attributed to water infiltration of the grooves of the textures as a result of capillary effects[39]. Hydrophobic behavior is observed for the bare Ti surface after FDTS modifying, and the WCA is observed to be 107° ± 2° (Fig. 2c), which is near the value after fluoroalkylsilane deposition, and can't be used as superhydrophobic surface absolutely. The surface became superhydrophobic after combination of chemical etching and FDTS modification, with its static contact angle increased greatly to 163° ± 2° (Fig. 2d). Fig.2(a-d) clearly reveals that the Titanium surface changed from hydrophic to superhydrophobic. The results indicate that both higher surface roughness and lower surface free energy play important roles in creating the superhydrophobic films. The wetting behavior of the resulting surface above can be theoretically explained by Cassie and Baxter equation[40],

$$\cos\theta_r = f_1 \cos\theta - f_2 \qquad \text{Eq. (1)}$$

where θ_r is the apparent contact angle on a rough surface, θ is the ideal contact angle on a smooth surface, and f_1 and f_2 are the fractional areas estimated for the solid and air on the surface, respectively (*i.e.* $f_1 + f_2 = 1$). θ_r (163°) and θ (107°) are the contact angles on a rough surface composed of chemical etched and FDTS-modified Ti substrate (Fig. 2d) and that on a smooth FDTS-modified Ti substrate respectively (Fig. 2c). From Eq. (1), we can find that the f_2 value of the rough surface with clusters is estimated to be 0.94 and f_1 is about 0.06. Obviously, it indicates that the air/water

interface effectively prevents the penetration of water droplets into the grooves, and the surface morphology plays a critical role in the preparation of a superhydrophobic Titanium surface.

In order to study the optimized fabrication, effects of experimental parameters (*e.g.*, H_2SO_4 concentration, the reaction temperature and time) on WCA are investigated. All the samples with contact angle mentioned in the following were modified with PDTS. Fig. 3(a) shows the WCA of different H_2SO_4 concentration treatment under the same temperature and time condition (120^{o}C and 30 min). The WCA of the surface treated with solution which contains 32% H_2SO_4 can only reach as high as 132° ± 2°, not reaching the standard of superhydrophobicity. When the concentration of H_2SO_4 is 72%, the WCA reaches a maximum value of 164° ± 1°, implying that this prepared surface could be used as a superhydrophobic surface absolutely. However, the WCA decreases to 111° ± 2° when the H_2SO_4 concentration reaches 92%. The relationship between WCA and the H_2SO_4 concentration is close to a convex curve. As shown in Fig. 3(b), variations in the WCA as a function of temperature treatment for Titanium surface at a condition of 72% H_2SO_4 for 30 minutes have been studied. The WCA of the surface treated with temperature of 80^{o}C reaches as high as 157° ± 2°, already reaching the standard of superhydrophobicity. When the temperature increases to 120^{o}C, the maximum value of WCA (164° ± 1°) appears, and then it decreased to 154° ± 8° under the temperature of 160^{o}C. Like WCA-concentration relationship, WCA-temperature relationship also roughly obeys the convex curve. This could attribute to the variation in the concentration of H_2SO_4, *i.e.*, the dilute H_2SO_4 solution and suitable temperature can make titanium corrode mildly, and produce a reasonable morphology of rough surface, which plays a very important role in superhydrophobicity. However, for a rigorous environmental corrosion (a higher temperature and more concentrated H_2SO_4), the oxidizing agents and certain multivalent metal ions could be formed on the Ti surface. It can even passivate and prevent Ti surface from further corrosion[41,42], thus deteriorates the surface roughness and reduces the WCA. Fig. 3(c) shows the change of WCA with different reaction time under the condition of 72% H_2SO_4 and 120^{o}C. The WCA of the

surface reached 155° ± 2° after 10 minutes' reaction, obtaining a significant superhydrophobicity. When the reaction time increased to 30 minutes, the WCA reached a maximum value of 164° ± 1°. But when the time was extended to 120 min, the WCA decreased to 150° ± 2°. The related analysis on the WCA-time relationship of superhydrophobicity of the films will be discussed further in the following section.

3.3. Surface morphology

From the above, it's clear that the etching time influences the surface wettability of the obtained surfaces, and the surface topography is one of the most important factors that determines the surface wettability. In order to explore the WCA-etching time relationship, the surface morphology of Titanium plates with different etching time was investigated by scanning electron microscopy (Fig. 4). Fuzzy farmland-like structure in Fig. 4(a) is formed on Titanium substrate after 10 minutes' etching. The possible reason is that the different crystal particle direction leads to different corrosion rate and morphology. When the etching time increases to 30 minutes, the farmland-like structure appears clearly, in which the vein-like and flake-like texture is formed (Fig. 4c). The inset of Fig. 4(c) indicates that pore diameter of the vein-like structure is 0.5-2 μm. By comparing Fig. 4(b) and Fig. 4(d), we can find that the fluctuating of etching 10 minutes and 30 minutes are both about 36 μm, but the bump structure after etching 30 minutes is more compact. Hence, the WCA of etching 30 minutes is larger than that of 60 minutes. However, when further etching is proceeded (more than 30 minutes), the particles with diameter of 50-80 μm are formed on the sample (Fig. 4e), and the fluctuation increases to 353 μm (Fig. 4f), which already exceeds the range of micro-nano scale. Thus, the WCA drops down. Fig. 4(g) shows that the diameter of particles had exceeded 400 μm, while Fig. 4(h) displays that the fluctuation increased to 1.23 mm, which indicates the structure is far away from the micro-nano scale.

3.4. Surface tension test

Mechanical durability is crucial to superhydrophobic surface under the real service condition. Tension test by using a uniaxial tensile machine is conducted to

determine the stretch resistance of the superhydrophobic surface. Fig. 5(a-b) shows the optical image of water droplet behavior on I-shape sample before and after the superhydrophobic treatment. Variation in WCA and sliding angle (SA) as a function of the tensile strain for the superhydrophobic surface is shown Fig. 5(c). From Fig. 5(c), we can find that the WCA decreased gradually and SA increased slowly with the increase of stretch strain, which means that the superhydrophobicity decreased slightly. It should be noted that the sample still has superhydrophobicity (157° ± 2° WCA and 6.7° ± 2.7° SA) after being stretched to the strain of 21%, indicating that the superhydrophobic sample has capacity for stretch resistance.

The stretch durability of the Ti superhydrophobicity surface is attributed to their morphology evolution. Fig. 6 demonstrates the SEM morphology of Ti superhydrophobic surface under different tensile strains. Obviously, more rough morphology with the increase of stretch strain can be formed, *i.e*, the width of grain boundary increased with the increase of stretch strain (see Fig. 6a-d), and interval of vein-like (Fig. 6e-h) or flake-like (Fig. 6i-l) structure in grain field increases correspondingly.

As for the flake-groove like structure, we can perform a two-step analysis to explore the relationship between the change of interval and the roughness. Firstly, we measure the interval of flake-groove like structure under different tension strains (Fig.7), and find that the interval of flake-groove structure increases linearly with tensile strain, *i.e*., 1.02 ± 0.17 μm (3%), 1.38 ± 0.17 μm (9%), 1.69 ± 0.24 μm (15%), and 2.19 ± 0.28 μm (21%), respectively. Afterwards, as illustrated in Fig. 8, we can analyze the roughness (r) of flake-like structure quantitatively, which is expressed as,

$$r = 1 + 2h / a \qquad \text{Eq. (2).}$$

where h is the depth of the groove, and a is the width of the interval. Based on the analysis above, we can find that the roughness gradually decreased with the increase of interval, and the increase of the strain leads to the decrease of roughness, thus the superhydrophobicity decreased slightly.

4. Conclusions

Superhydrophobic surfaces with farmland-like texture on Titanium substrate were fabricated by means of a chemical etching and surface self-assembly method. The results indicated that the optimum condition is H_2SO_4 concentration of 72%, temperature of 120^oC and time duration of 30 minutes. XRD shows TiO was generated on the sample which was conducive to the surface self-assembly. The SEM of Titanium plates with different etching time well reflected the change in WCA with the etching time. Moreover, the surface tension tests show that the fabricated superhydrophobic surface possessed good stretch resistance. The proposed method is feasible to be applied in practice of superhydrophobic Titanium surfaces due to its facile process and short cycle.

Acknowledgments

We gratefully acknowledge support of this work by the National Natural Science Foundation of China (11202178, 11275150 and 11435010) and Natural Science Foundation of Hunan Province (14JJ3082).

References

1 D. Quéré, *Annu. Rev. Mater. Res*, 2008, **38**, 71-99.
2 S. Nishimoto and B. Bhushan, *Rsc Adv*, 2013, **3**, 671-690.
3 P. Ragesh, V. A. Ganesh, S. V. Nair and A. S. Nair, *J. Mater. Chem. A*, 2014, **2**, 14773-14797.
4 R. Fürstner, W. Barthlott, C. Neinhuis and P. Walzel, *Langmuir*, 2005, **21**, 956-961.
5 S. Li, M. Jin, C. Yu and M. Liao, *Colloid Surf. A- Physicochem. Eng. Asp*, 2013, **430**, 46-50.
6 Y. Zhou, M. Li, B. Su and Q. Lu, *J. Mater. Chem*, 2009, **19**, 3301-3306.
7 C. Liu, F. Su and J.Liang, *RSC Adv*, 2014, **4**, 55556-55564.
8 Y. Cheng, S. Lu, W. Xu and H. Wen, *RSC Adv*, 2015, **5**, 15387-15394.
9 M. Ruan, W. Li, B. S. Wang and B.W. Deng, *Langmuir*, 2013, **29**, 8482-8491.
10 X. Zhan, Y. Yan, Q. Zhang and F. Chen, *J. Mater. Chem. A*, 2014, **2**, 9390-9399.
11 S. Farhadi, M. Farzaneh and S. Kulinich, *Appl. Surf. Sci*, 2011, **257**, 6264-6269.
12 F. Liu, S. L. Wang, M. Zhang, M. L. Ma, C. Y. Wang and J. Li, *Appl. Surf. Sci*, 2013, **280**, 686-692.
13 C. Wang, *et al. Adv. Powder Technol*, 2014, **25**, 530-535.
14 Q. F. Sun, Y. Lu, J. Li and J. Cao, *Key Eng. Mater*, 2014, **609**, 468-471.

15 J. Park, H. Lim, W. Kim and J. S. Ko, *J. Colloid Interface Sci*, 2011, **360**, 272-279.

16 H. Y. Ji, G. Chen, J. Yang, J. Hu, H. J. Song and Y. T. Zhao, *Appl. Surf. Sci*, 2013, **266**, 105-109.

17 H. M. Kim, S. Sohn and J. S. Ahn, *Surf. Coat. Technol*, 2013, **228**, S389-S392.

18 J. Ou, W. Hu, M. Xue, F. Wang and W. Li, *ACS Appl. Mater. Interfaces*, 2013, **5**, 3101-3107.

19 W. Y. Liu, Y. T. Luo, L. Y. Sun, R. M. Wu, H. Y. Jiang and Y. J.Liu, *Appl. Surf. Sci*, 2013, **264**, 872-878.

20 J. L. Song, Y. Lu, S. Huang, X. Liu, L. B. Wu and W. J. Xu, *Appl. Surf. Sci*, 2013, **266**, 445-450.

21 J. Liang, Y. Zhou, G. H. Jiang, R. J. Wang, X. H. Wang, R. B. Hu and X. G. Xi, J. *Text. Inst*, 2013, **104**, 305-311.

22 M. E. Yazdanshenas and M. Shateri-Khalilabad, *Ind. Eng. Chem. Res*, 2013, **52**, 12846-12854.

23 B. Wang, Y. B. Zhang, W. X. Liang, G. Y. Wang, Z. G. Guo and W. M. Liiu, *J. Mater. Chem. A*, 2014, **2**, 7845-7852.

24 J. Victor, D. Facchini and U. Erb, *J. Mater. Sci*, 2012, **47**, 3690-3697.

25 Q. F. Xu, B. Mondal and A. M. Lyons, *ACS Appl. Mater. Interfaces*, 2011, **3**, 3508-3514.

26 W. Barthlott and C. Neinhuis, *Planta*, 1997, **202**, 1-8.

27 L. Feng, S. H. Li, Y. S. Li, H. J. Li, L. J. Zhang, J. Zhai, Y. L. Song, B. Q. Liu, L. Jiang and D. B. Zhu, *Adv. Mater*, 2002, **14**, 1857-1860.

28 R. P. Evershed, R. Berstan, F. Grew, M. S. Copley, A. J. H. Charmant, E. Barham, H. R. Mottram and G. Brown, *Nature*, 2004, **432**, 36.

29 T. L. Sun, L. Feng, X. F. Gao and L. Jiang, *Acc. Chem. Res*, 2005, **38**, 644-652.

30 Q. F. Cheng, M. Z. Li, Y. M. Zheng, B. Su, S. T. Wang and L. Jiang, *Soft Matter*, 2011, **7**, 5948-5951.

31 Q. F. Cheng, M. Z. Li, F. Yang, M. J. Liu, L. Li, S. T. Wang and L. Jiang, *Soft Matter*, 2012, **8**, 6740-6743.

32 Q. F. Cheng, L. Jiang and Z. Y. Tang, *Acc. Chem. Res*, 2014, **47**, 1256−1266.

33 Y. M. Zheng, H. Bai, Z. B. Huang, X. L. Tian, F. Q. Nie, Y. Zhao, J. Zhai and L. Jiang, *Nature*, **463**, 640-643.

34 F. Su and K. Yao, *ACS Appl. Mater. Interfaces*, 2014, **6**, 8762-8770.

35 J. Yang and W. Li, *J. Alloys Compd*, 2013, **576**, 215-219.

36 L. J. Li, Y. Z. Zhang, J. L. Lei, J. X. He, R. Lv, N. B. Li F. S. Pan, *Corros. Sci*, 2014, **85**, 174-182.

37 M. Guo, Z. Kang, W. Li and J. Zhang, *Surf. Coat. Technol*, 2014, **239**, 227-232.

38 E. Fadeeva, V. K. Truong, M. Stiesch, B.N. Chichkov, R. J. Crawford, J. Wang and E. P. Ivanova, *Langmuir*, 2011, **27**, 3012-3019.

39 Y. Tian and L. Jiang, *Nat. Mater*, 2013, **12**, 291-292.

40 S. T. Wang, L. Feng and L. Jiang, *Adv. Mater*, 2006, **18**, 767-770.

41 Z. Y. Jiang, J. T. Wang, Q. Hu and S. Y. Huang, *Corros. Sci*, 1995, **37**, 1245-1252.

42 A. Robin, J.L. Rosa, H.R.Z. Sandim, J. Appl. Electrochem, 2001, 31, 455-460.

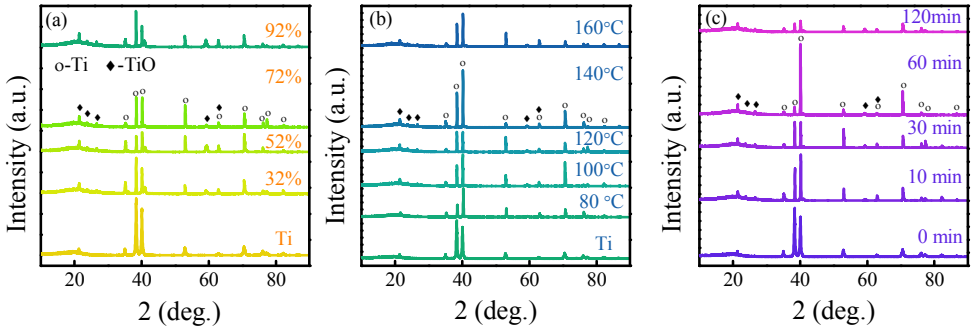

Fig. 1. XRD patterns of Titanium surfaces under different chemical etching conditions: (a) H_2SO_4 concentration (with 120 ^oC and 30 min), (b) Temperature (with 72% H_2SO_4 and 30 min), and (c) Time (with 72% H_2SO_4 and 120 ^oC)

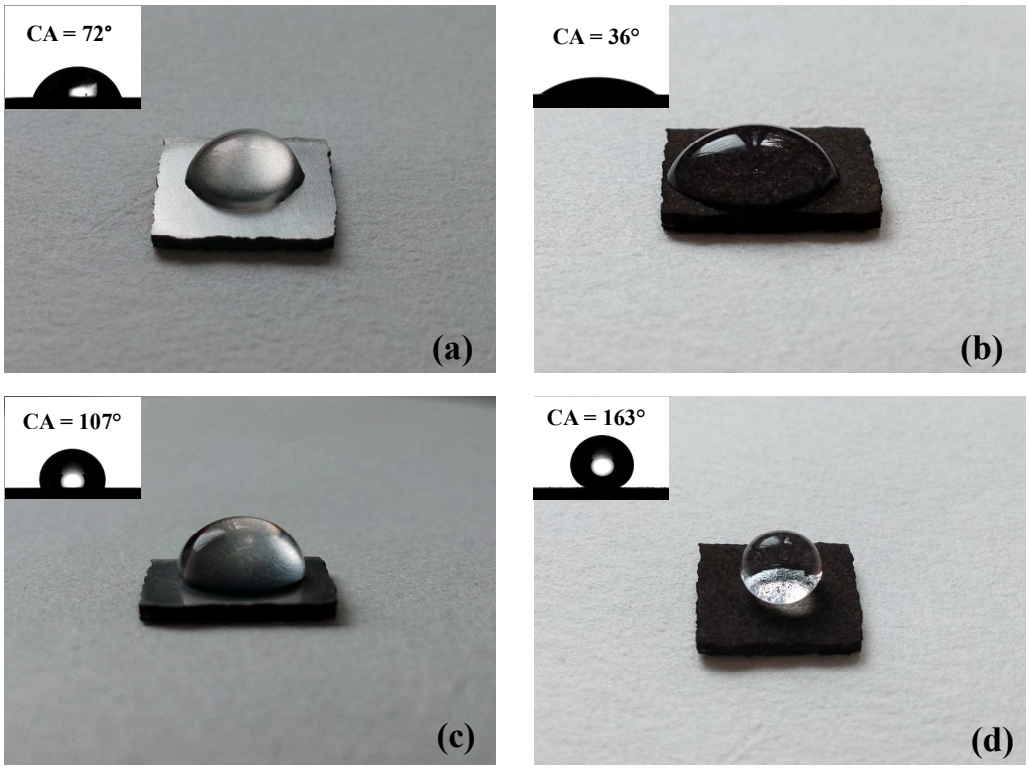

Fig. 2. Photographs of water droplets on Ti substrates after different treatments: (a) as-prepared Ti substrate, (b) chemical etched Ti substrate, (c) FDTS-modified Ti substrate, (d) chemical etched and FDTS-modified Ti substrate. The insets are the contact angle photos of water droplet covering the surfaces.

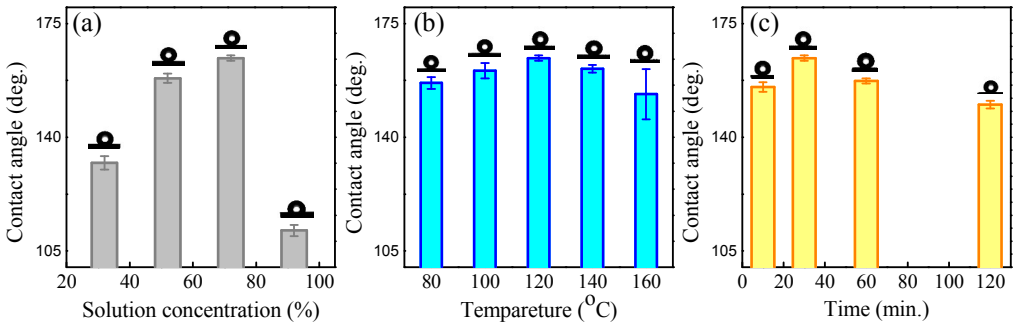

Fig. 3 Water contact angle of Titanium surface under different chemical etching conditions: (a) H_2SO_4 concentration (with 120 °C for 30 minutes), (b) Temperature (with 72% H_2SO_4 for 30 minutes), and (c) Time (with 72% H_2SO_4 and 120 °C). The insets are optical photographs of water droplets on different Ti surfaces.

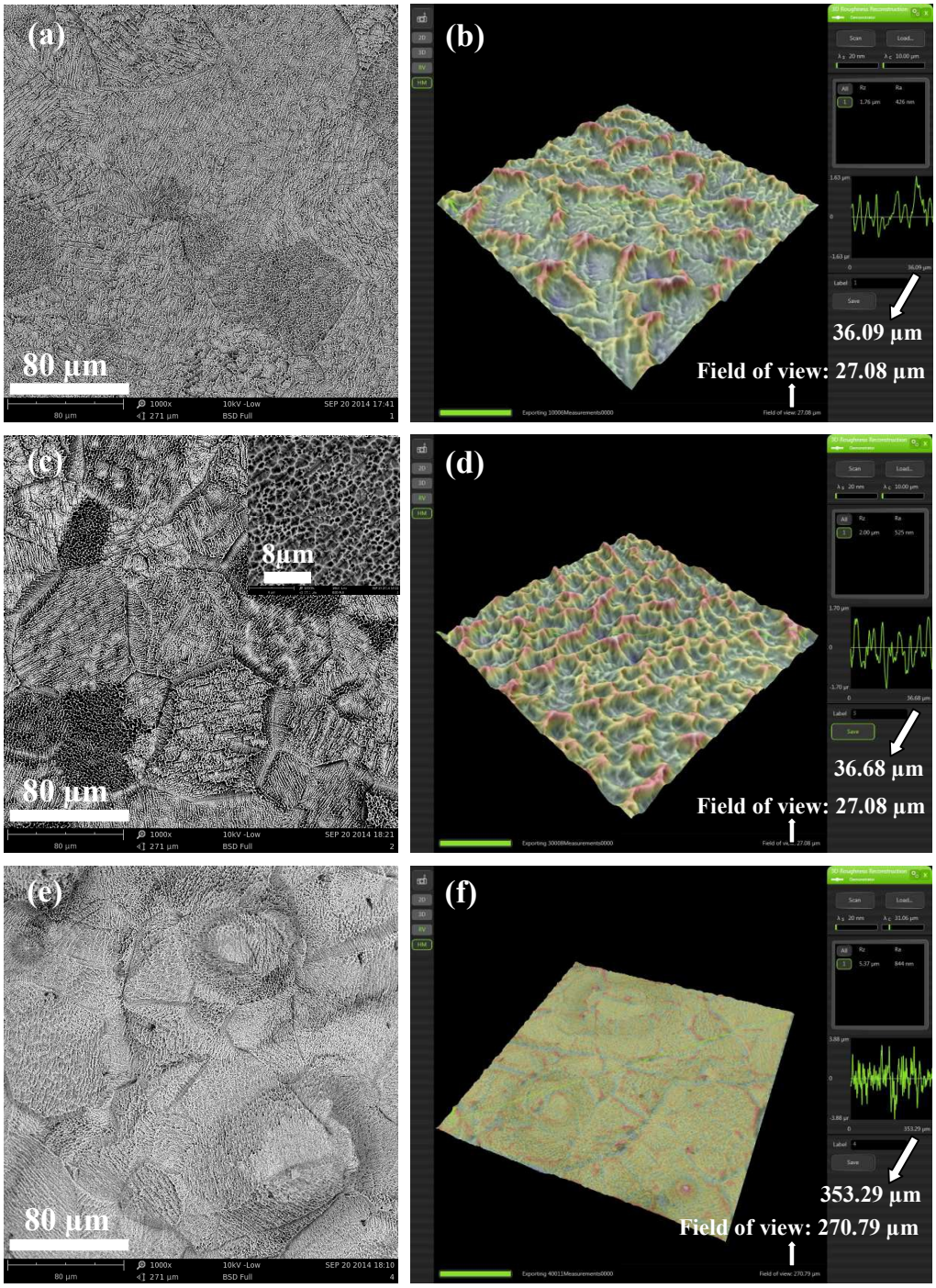

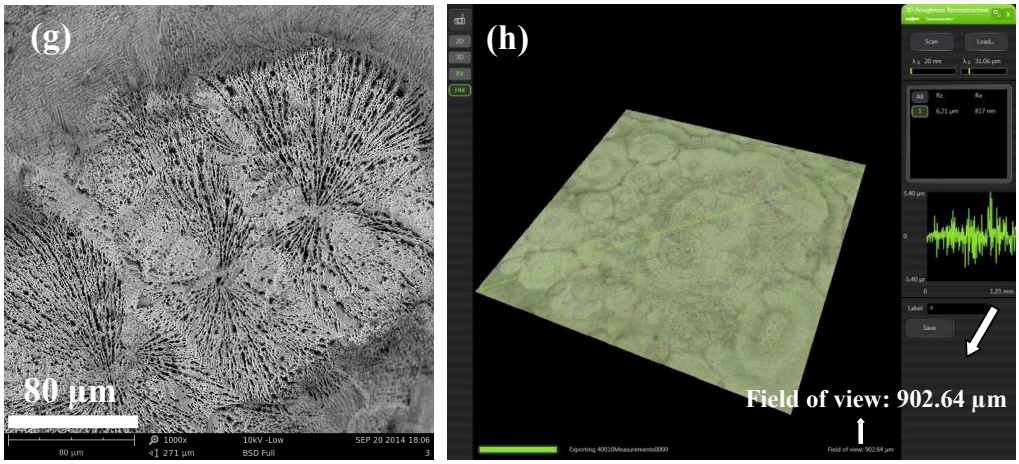

Fig. 4 SEM and 3D images of Titanium substrate after being etched at a solution containing 72% H_2SO_4 at 120^{o}C for (a, b)10 min, (c, d) 30 min, (e, f) 60 min, and (g, h) 120 min.

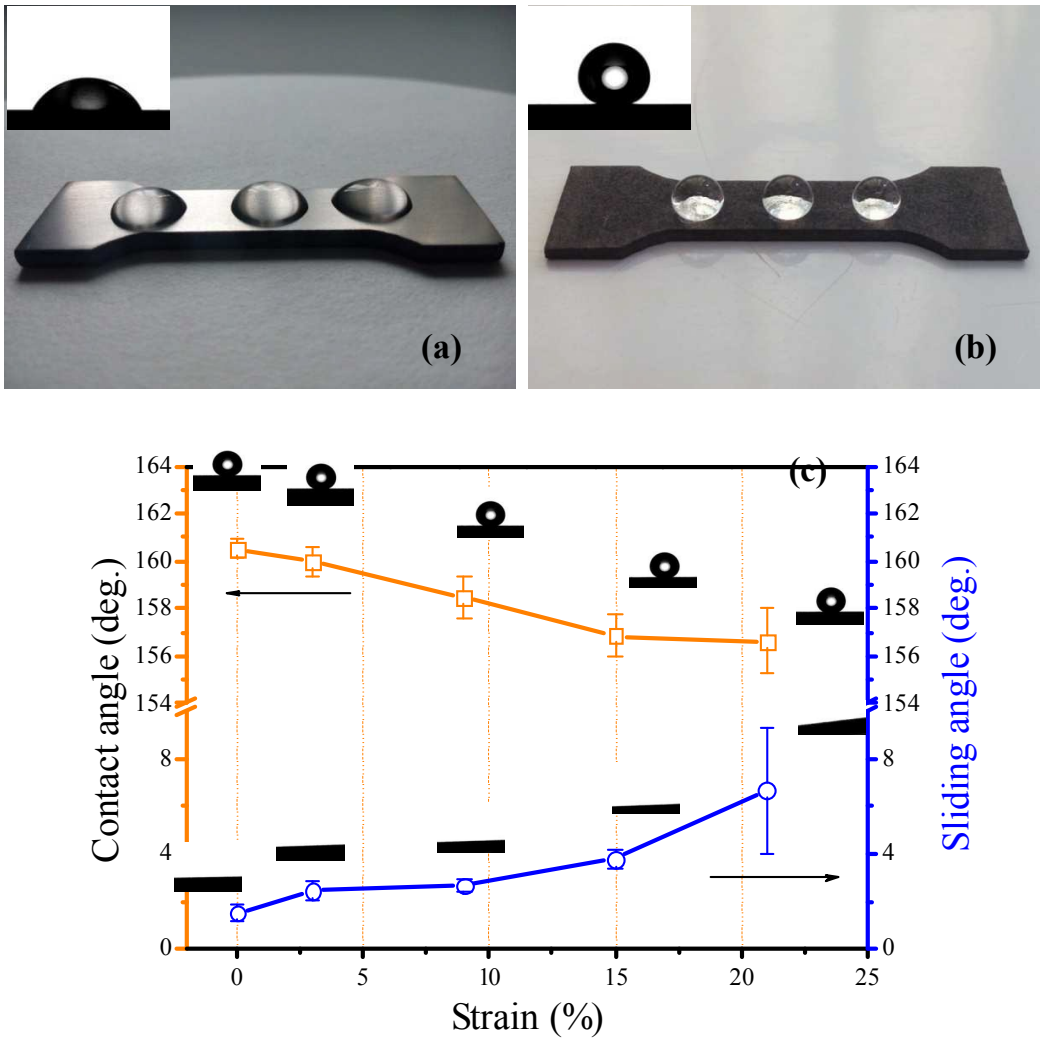

Fig. 5. Optical image of water droplets on (a) Ti substrate, (b) superhydrophobic Titanium surface; (c) Water contact angle and sliding angle of superhydrophobic Ti samples under different tension strains. The insets are the photos of water droplet covering and sliding on the surfaces, respectively.

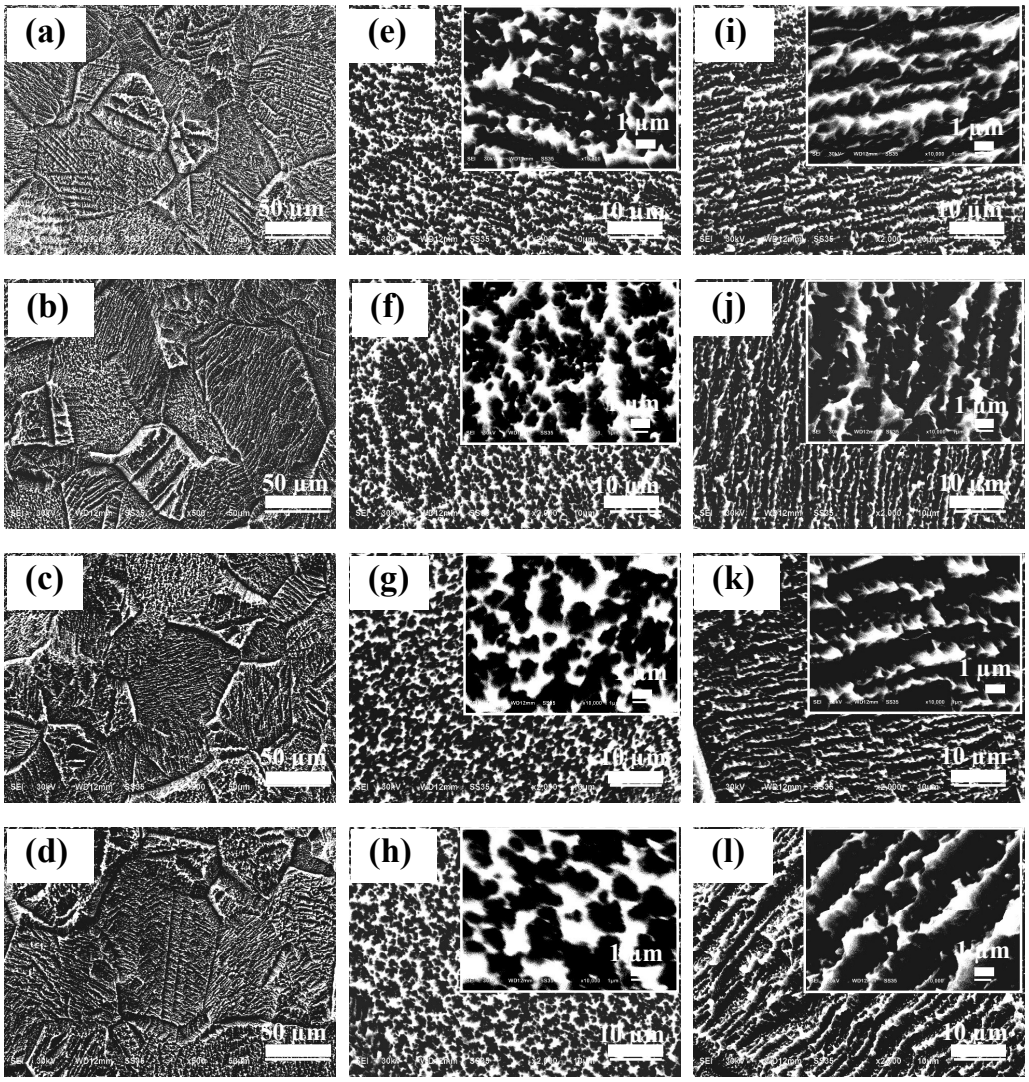

Fig. 6. SEM images of superhydrophobic Ti samples after different strains: (a, e, i) 3%, (d, e, f) 9%, (g, h, i) 15%, and (j, k, m) 21%; The insets are the higher magnification SEM images.

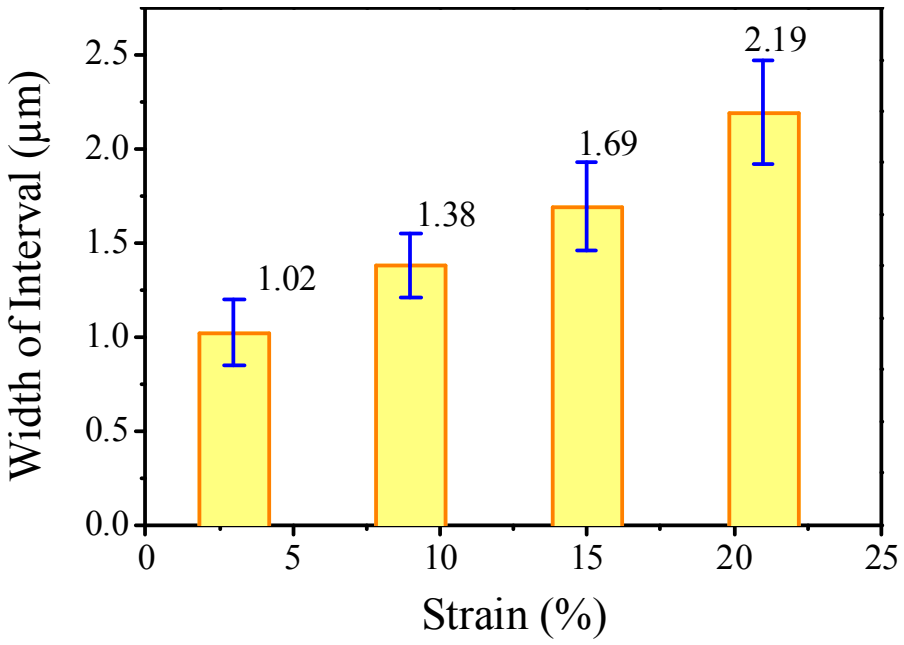

Fig. 7. The interval of flake-groove structure on superhydrophobic Ti surface as a function of tension strains (from 3% to 21%)

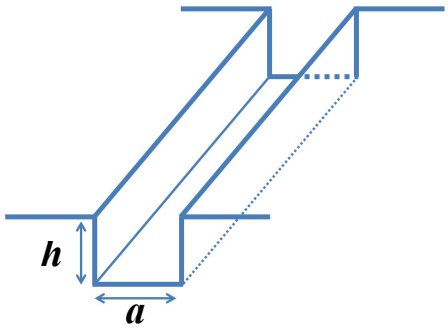

Fig. 8. Illustration diagram of the flake-groove structure on superhydrophobic surface of Ti sample